ELSEVIER

Journal of Power Sources 97–98 (2001) 366–370

JOURNAL OF POWER SOURCES

www.elsevier.com/locate/jpowsour

Improved cycle performance of orthorhombic $LiMn_{0.95-x}M_xCr_{0.05}O_2$; M = Al, Ga, Yb and In, synthesized by hydrothermal technique

Takeshi Sakurai*, Takashi Kimura, Tadashi Sugihara

Microelectronics Laboratories, Central Research Institute, Mitsubishi Materials Corporation, 1-297 Kitabukuro, Omiya, Saitama 330-8508, Japan

Received 6 June 2000; received in revised form 13 February 2001; accepted 19 February 2001

Abstract

The effect of chemical substitution on improving cycle performance of orthorhombic $LiMnO_2$ (o-$LiMnO_2$) was studied at the nominal compositions of $LiMn_{0.95-x}M_xCr_{0.05}O_2$; M = Al, Ga, Yb and In, $0.01<x<0.07$. Samples obtaining single phase were synthesized by hydrothermal technique. As the result of studies, $LiMn_{0.92}In_{0.03}Cr_{0.05}O_2$ was confirmed as the optimum composition. The crystal structure refinement showed that chemical substitution varied the average ionic radii of cation sites in o-$LiMnO_2$. The ratio of average ionic radius at Mn site to that of Li site of the optimum compound was 0.87. This value was larger than that of no-substituted $LiMnO_2$; 0.84. TEM observation revealed that stacking faults were observed in the $LiMn_{0.92}In_{0.03}Cr_{0.05}O_2$ grains. It is assumed that these two factors, controlling ionic radii and introducing stacking faults, are key parameters for improving cycle performance. However X-ray diffraction data and discharge curves suggested that phase transformation from orthorhombic to cubic spinel occurred during charge–discharge cycle.

Keywords: Orthorhombic $LiMnO_2$; Substitution effect; In; Cr; Cycle property

1. Introduction

Lithium manganese oxide compounds are major candidates for low cost and safe cathode material of the lithium rechargeable batteries. Batteries utilizing $LiMn_2O_4$ compound having a spinel structure has already commercialized in some markets. Comparing to $LiCoO_2$ or $LiNiO_2$ based cathode materials, spinel compound are recognized for their superiority for the safety program and low cost. However, the specific capacity of 120 mAh/g class is thought to be an inferiority of the lithium manganese compound. So, other manganese-based compounds exhibiting higher specific capacity are examined. Ozuku et al. reported LT-$LiMnO_2$ exhibited high capacity up to 190 mAh/g [1]. This compound was thought to be an orthorhombic $LiMnO_2$ (o-$LiMnO_2$) with many stacking faults. Croguennec et al. reported that active material having small grain size under 1 μm and stacking faults induced moderately enhanced the discharge capacity up to 200 mAh/g, but degraded the retentively of the specific capacity [2]. According to their crystal structure analysis, atomic disposition around the stacking fault area seemed to be similar to that of spinel structure [3]. On the other hand, Kotchau et al. reported that o-$LiMnO_2$ exhibited poor cycle performance causing the irreversible phase transformation which occurred from orthorhombic to cubic spinel related structure during first charge [4]. It is assumed that local spinel like atomic disposition would behave as a starting point of phase transformation to spinel structure. So, if an o-$LiMnO_2$ phase with small grain size and with moderate stacking faults is successfully synthesized, specific discharge capacity and cycle performances are supposed to be improved.

In this study, the effect of substitution on the phase stability was examined by controlling the ionic radii of cation site at the nominal compositions of $LiMn_{0.95-x}M_xCr_{0.05}O_2$; M = Al, Ga, Yb and In, $0.01 < x < 0.07$. It is supposed that controlling cation ionic radius would stabilize o-LiMnO2 structure. Key parameters of improving cycle performance were discussed.

2. Experimental procedure

Substituted o-$LiMnO_2$ samples; $LiMn_{0.95-x}M_xCr_{0.05}O_2$, were synthesized by hydrothermal technique [5] from a mixture of precursor and LiOH monohydrate. The way of

* Corresponding author.

0378-7753/01/$ – see front matter
PII: S0378-7753(01)00762-5

precursor preparation was different among the combinations of additive elements; M. When M = Al and Ga, Mn_2O_3 and other additive powders, which were Cr_2O_3, $Al(OH)_3$ (3N, Soekawa chemical Co., each) or Ga_2O_3 (3N, Mitsubishi materials Co.), were weighed for the compositions of $Mn_{0.95-x}M_xCr_{0.05}O_2$; $x = 0.01$, 0.02, 0.03, 0.05 and 0.07, and mixed in an agate mortar. After that, they were pressed into disk-shaped pellets with 20 mm diameter and 3 mm thickness, and fired at 800°C for 10 h under the air using a setter made of ZrO_2. Heat up and cooling down procedure was performed by the rate of 200°C/h, respectively. Resulted pellets were grinded and passed the sieve with the aperture size of 500 μm. X-ray diffraction analysis revealed that powders exhibited single phase of Mn_2O_3 structure at any composition. Li-excess mixture of precursor and LiOH monohydrate, that is Li/(Mn + M + Cr) = 40 in molecular ratio was settled in the Teflon® beaker and hydrothermally processed at 230°C and 28 kgf/cm^2 for 6 h using autoclave (Taiatsu Co.). Before heating up, the residual air in the pressure-vessel was substituted by Ar gas in order to prevent the oxidation of Mn^{3+}. The products were washed with distilled water to eliminate residual LiOH. And then they were dried in vacuum desiccators at room temperature using P_2O_5 as a desiccant. When M = In and Yb, Li-excess mixture was consisted of LiOH, $InCl_3$,$4H_2O$ or $Yb(CH_3COO)_3$,$4H_2O$ (3N, Wako junyaku Co, each) and $Mn_{0.95-x}Cr_{0.05}O_z$ precursors, whose x were 0.01, 0.02, 0.03, 0.05 and 0.07. And they were treated by hydrothermal process with the same condition.

In the hydrothermal synthesis, starting materials were selected from the point of solubility into the alkali solution under the hydrothermal conditions. For example, when In_2O_3 powders were used as starting material, X-ray diffraction data exhibited sharp In_2O_3 peaks at the nominal composition of $LiMn_{0.94}In_{0.01}Cr_{0.05}O_2$. Because, In_2O_3 is so stable as to hardly dissolve in the alkali solution. On the other hand, when $InCl_3$,$4H_2O$ powders were used, X-ray diffraction data exhibited no impurity phase.

Resulted powders were characterized by XRD. (Mac Science, XMP18), TEM (JEOL, TEM-2010F) observations and cycle performances. Chemical compositions were analyzed by ICP method using ICAP55 (Nihon Jareleash).

Charge and discharge properties were measured using three electrodes open cells assembled under the dry Ar atmosphere. The preparation of working electrode was based on Richard's method [6]. Counter and reference electrodes were made of Li foil. The electrolyte composition was 1.0 M of $LiPF_6$ in a mixture of ethylene carbonate (EC) and propylene carbonate (PC) in a volume ratio of 1:1. Open cells were charged by constant current and constant voltage mode and discharged by constant current mode. Cathode electrodes were charged up to 4.3 V versus Li/Li$^+$ with current density of 20 mA/g-cathode material. After the potential reached to 4.3 V versus Li/Li$^+$, current density was decreased continuously to keep the same potential until the scheduled period had passed. Then, they were discharged down to 2.5 V versus Li/Li$^+$ with current density of 10 mA/g-cathode material. The current densities at charge and discharge were determined in order to be equivalent to the C/8 rate and C/16 rate, respectively.

3. Results and discussions

The formed phases were confirmed by X-ray diffraction. No impurity phase was detected in the substitute range up to $x = 0.07$ by X.R.D. for the case of M = Al and Ga. Oxide impurities were obtained in the content range more than $x = 0.05$ and 0.03 for the case of M = In and Yb, respectively. Single-phase samples seemed to be obtained as a function of the average ionic radii at Mn site. Further characterizations were performed for the samples obtaining single phase.

Fig. 1 shows cycle performances of o-$LiMn_{0.95-x}M_xCr_{0.05}O_2$ samples synthesized by hydrothermal technique. Specific discharge capacities are monotonically decreased for the samples; M = Al, Ga and Y, which reduce the average ionic radius at Mn site. The other samples, M = In and Yb, cycle performance are found to be improved in the initial stage. For the M = In case, specific discharge capacity is maximized up to 150 mAh/g at 10th cycle and the capacity is maintained up to 50th cycle. After that, the capacity is monotonically reduced down to 110 mAh/g at 100th cycle. For the M = Yb case, specific discharge capacity is maximized up to 175 mAh/g at 25th cycle and the capacity is monotonically reduced down to 110 mAh/g at 100th cycle.

Fig. 2 shows the TEM image using dark field technique. This image reveals many contrasted parallel stripes in a

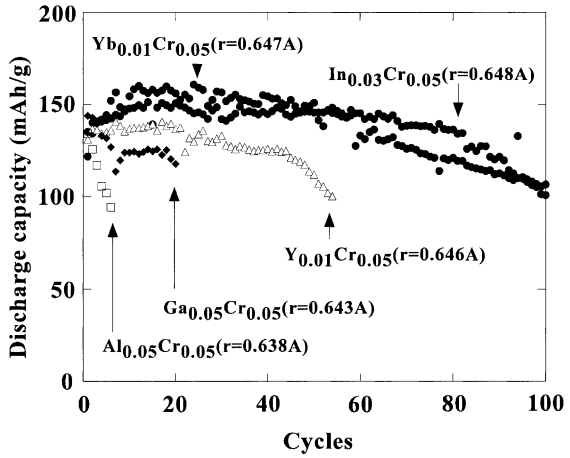

Fig. 1. Cycle performance of $LiMn_{0.95-x}M_xCr_{0.05}O_2$ samples obtained by hydrothermal technique where M = Al, Ga, In, Y and Yb. Substituting composition and its average ionic radius is noted in the figure. The cathode electrode was charged up to 4.3 V vs. Li/Li$^+$ with current density of 20 mA/g-cathode material. After potential reached to 4.3 V vs. Li/Li$^+$, current density was decreased continuously to keep the same potential until the scheduled period had passed. Then, it was discharged down to 2.5 V vs. Li/Li$^+$ with current density of 10 mA/g-cathode material.

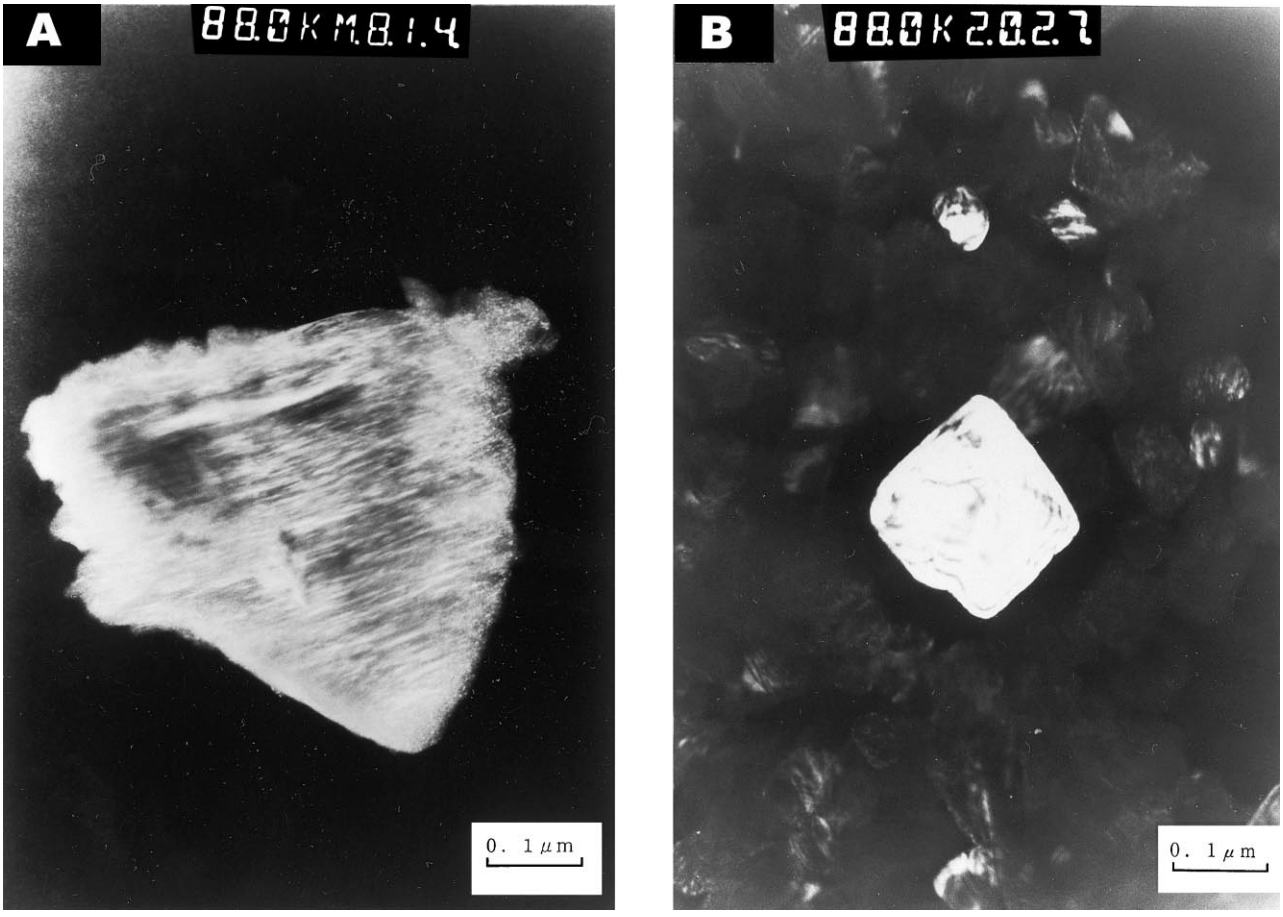

Fig. 2. The dark field image of TEM observation for the $LiMn_{0.92}In_{0.03}Cr_{0.05}O_2$ grains (A) and no substituted $LiMnO_2$ grains (B), which are obtained by hydrothermal technique. Contrasted stripes suggest the existence of stacking faults of crystal structure.

$LiMn_{0.92}In_{0.03}Cr_{0.05}O_2$ grain. These stripes suggest the existence of stacking faults of crystal structure. So, this seems to be consistent with Croguennec's result [3]. They reported that good cycle performance was observed in the samples, which were identified to include stacking faults in grains. It can be said that cation substitution performed by hydrothermal technique enables to introduce the stacking faults in grains.

Table 1 shows the results of analyzed chemical compositions and the site preferences estimated by Rietveld

Table 1
The results of analyzed chemical compositions and the site preferences estimated by Rietveld refinement using RIETAN [7][a]

Sample no.	1	2	3
Nominal composition	$LiMn_{0.92}Cr_{0.05}In_{0.03}O_2$	$LiMn_{0.9}Cr_{0.05}Al_{0.05}O_2$	$LiMnO_2$
Analyzed composition	$Li_{0.92}MnIn_{0.03}Cr_{0.05}O_2$	$Li_{1.036}Mn_{0.89}Cr_{0.044}Al_{0.03}O_2$	$Li_{1.06}Mn_{0.92}O_2$
Rwp (%)	13.6	14.2	9.8
Site preferences			
Li-site	$Li_{0.86}Mn_{0.06}In_{0.03}Cr_{0.05}$	$Li_{0.928}Mn_{0.05}Cr_{0.022}$	$Li_{1.0}$
Mn-site	$Mn_{0.94}Li_{0.06}$	$Mn_{0.84}Li_{0.108}Cr_{0.022}Al_{0.03}$	$Mn_{0.92}Li_{0.06}$
Average ionic radius			
Li-site (A)	0.747	0.751	0.760
Mn-site (A)	0.652	0.653	0.639
Ratio(Mn site/Li site)	0.873	0.869	0.841
Stacking fault	Yes	No	No
Cycle performance	Improved	Not improved	Not improved

[a] Improved cycle performance was obtained when both controlling the average ionic radius and introducing the stacking faults are achieved.

refinement using RIETAN [7]. 3 samples were examined. Sample 1 is $LiMn_{0.92}In_{0.03}Cr_{0.05}O_2$, which shows improved cycle performance. The ratio of average ionic radius at Mn site to that of Li site is 0.87, using the refined site preferences; $(Li_{0.86}Mn_{0.06}In_{0.03}Cr_{0.05})(Mn_{0.94}Li_{0.06})O_2$, and the ionic radius [8]. Sample 2 is $LiMn_{0.9}Al_{0.05}Cr_{0.05}O_2$. The value of ionic radius ratio is close to that of sample 1, but cycle performance is not improved because of the non-existence of stacking faults. Sample 3 is the no-substituted *o*-$LiMnO_2$, whose the ionic radius ratio is 0.84. Both controlling the average ionic radius and introducing the stacking faults are key parameters to improve the cycle performance.

Fig. 3 shows the X-ray diffraction patterns of cathode electrodes made of $LiMn_{0.92}In_{0.03}Cr_{0.05}O_2$ sample. "O" indicates the peaks, which belong to the orthorhombic $LiMnO_2$. "C" indicates the peaks, which belong to the cubic spinel $LiMn_2O_4$. "Al" indicates peaks caused by Aluminum mesh, which are used for current collectors of electrodes. The orthorhombic phase is dominant in the samples; "before discharging" and "after two cycles discharged". The cubic spinel phase becomes dominant in other samples. It can be said that the phase transformation from orthorhombic to cubic spinel occurred in the charge discharge cycles.

Fig. 4 shows the relationship between discharge capacity and voltage. A plateau around 4 V versus Li/Li^+ begins to

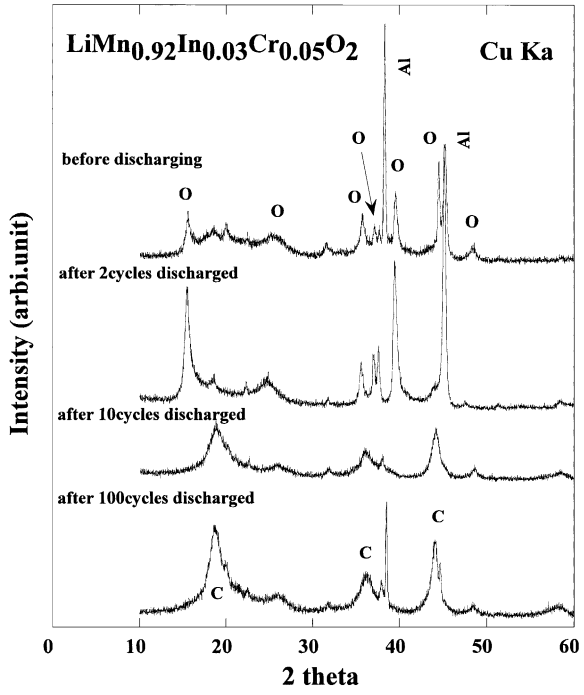

Fig. 3. The change of X-ray diffraction patterns of $LiMn_{0.92}In_{0.03}Cr_{0.05}O_2$ cathode electrode during charge and discharge cycle. Patterns are of as prepared electrode, after two cycles discharged, after ten cycles discharged and after 100 cycles discharged, respectively "O" indicates the peaks, which belong to the orthorhombic $LiMnO_2$. "C" indicates the peaks, which belong to the cubic spinel $LiMn_2O_4$. "Al" indicates peaks caused by Aluminum mesh, which are used for current collectors of electrodes. The phase transformation from orthorhombic to cubic spinel is observed.

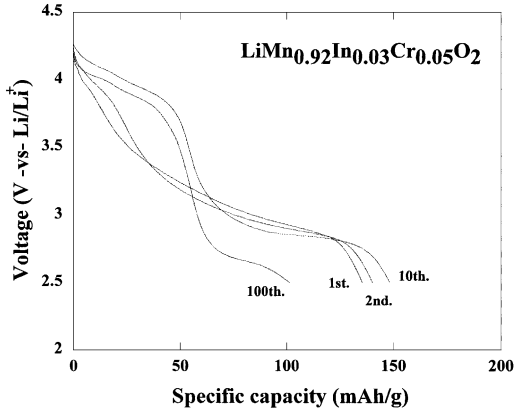

Fig. 4. The relationship between discharge capacity and voltage. Discharge curves are of 1st discharged, after two cycles discharged, after ten cycles discharged and after 100 cycles discharged, respectively. A plateau around 4 V versus Li/Li^+ appears even in the second discharge process. It suggests that the phase transformation from orthorhombic to cubic spinel quickly occurs.

appear in the second discharge process. It is considered that the plateau causes to the cubic spinel, because there is no other manganese based active material exhibiting 4 V reaction. As the capacity of the cubic spinel is added to that of orthorhombic compound, the total capacity is increased at the early stage of charge discharge cycle. In the middle stage, the increased capacity causing to cubic spinel compensates for the capacity loss of orthorhombic compound due to the reduction of volume fraction. So, specific capacity looks to be kept in Fig. 1. The capacity causing to *o*-$LiMnO_2$ still exists at 100th discharged sample. It is thought that the phase transformation occurs quickly, but the orthorhombic related structure is still reserved in the cubic spinel. It is thought that the heterogeneity of spinel structure causes the broadened X-ray diffraction peaks and the saturated capacity around 60 mAh/g. Therefore, perfect phase transformation form *o*-$LiMnO_2$ structure to cubic spinel hardly occurs during the cycle. It is suspected that more improved cycle performance would be realized. If the conditions of controlling the phase transformation were found, *o*-$LiMnO_2$ structure was stabilized.

4. Conclusions

The effect of substitution on the phase stability was studied by controlling the ionic radii of cation site at the nominal compositions of $LiMn_{0.95-x}M_xCr_{0.05}O_2$; M = Al, Ga, Yb and In, $0.01 < x < 0.07$. Two key parameters for improving cycle performance of *o*-$LiMnO_2$ were revealed. They are: controlling average ionic radii at cation sites and introducing stacking faults in grains. Cycle performance was effectively improved when the nominal composition was $LiMn_{0.92}In_{0.03}Cr_{0.05}O_z$. But X-ray diffraction data and discharge curves suggested that phase transformation from orthorhombic to cubic spinel occurred during

charge–discharge cycle. It was thought that controlling average ionic radii at cation sites and introducing stacking faults in grains were not sufficient conditions but necessary conditions. If the conditions of controlling the phase transformation were found, stabilized *o*-$LiMnO_2$ structure would achieve more improved cycle performance.

Acknowledgements

This work was performed by Mitsubishi Materials Corporation, under the management of the Micromachine Center, as the Industrial Science and Technology Frontier Program ''Research and Development of Micromachine Technology'' of MITI, supported by the New Energy and Industrial Technology Development Organization. Authors thank Shin Tsuchiya for helpful discussions and Hirokazu Akiyama for TEM observation.

References

[1] T. Ozuku, A. Ueda, T. Hirai, Chem. Express 7 (1992) 193–196.
[2] L. Croguennec, P. Deniard, R. Brec, J. Electrochem. Soc. 144 (1997) 3323–3330.
[3] L. Croguennec, P. Deniard, R. Brec, A. Lecerf, J. Mater. Chem. 7 (1997) 511–516.
[4] I.M. Kotchau, J.R. Dahn, J. Electrochem. Soc. 145 (1998) 2672–2677.
[5] M. Tabuchi, et. al., Solid State Ionics 89 (1996) 53–63.
[6] M.N. Richard, I. Koetschau, J.R. Dahn, J. Electrochem. Soc. 144 (1997) 554–557.
[7] F. Izumi,The Rietveld Method, in: R.A.Young (Ed.), Oxford University Press, Oxford, 1993 (Chapter 13).
[8] R.D. Shannon, Acta Cryst. A 32 (1976) 751–767.